JOURNAL OF GEOPHYSICAL RESEARCH, VOL. 103, NO. A11, PAGES 26,833-26,849, NOVEMBER 1, 1998

Interplanetary Lyman α observations from Pioneer Venus over a solar cycle from 1978 to 1992

Wayne R. Pryor,[1] Scott J. Lasica,[1] A. Ian F. Stewart,[1] Doyle T. Hall,[1] Sean Lineaweaver,[1] William B. Colwell,[1] Joseph M. Ajello,[2] Oran R. White,[3] and W. Kent Tobiska[4]

Abstract. The Pioneer Venus Orbiter ultraviolet spectrometer (PVOUVS) routinely obtained interplanetary hydrogen Lyman α data while viewing ecliptic latitudes near 30°S from 1978 to 1992 (during solar cycles 21 and 22). We describe "hot" models for this interplanetary Lyman α data that include the solar cycle variation of (1) the solar flux, as a function of latitude and longitude; (2) the radiation pressure on hydrogen atoms; (3) the solar wind flux; (4) the solar EUV flux; and (5) the multiple scattering correction to an optically thin radiative transfer model. These models make use of solar radiation flux parameters (solar wind, solar EUV, and solar Lyman α) from spacecraft and ground-based solar proxy observations. Comparison of the upwind data and model indicates that the ratio of the solar Lyman α line center flux (responsible for the interplanetary signal) to the observed solar Lyman α integrated flux is constant to within ~20%, with an effective line width near 1.1 Å. Averaging the solar radiation pressure and hydrogen atom lifetime over 1 year before the observation reproduces the upwind intensity time variation but not the downwind. A better fit to the downwind time series is found using the 1 year average appropriate for the time that the atoms passed closest to the sun. Solar Lyman α measurements from two satellites are used in our models. Upper Atmosphere Research Satellite (UARS) solar Lyman α measurements are systematically higher than Solar Mesosphere Explorer (SME) values and have a larger solar maximum to solar minimum ratio. UARS-based models work better than SME-based models in fitting the PVOUVS downwind time series Lyman α data.

1. Introduction

The interplanetary Lyman α glow comes from solar Lyman α that has been scattered by hydrogen atoms in the very local interstellar medium. At a distance of perhaps 30 AU upwind from the Sun, well inside the solar wind termination shock, these hydrogen atoms are currently described by a temperature $T \approx 8000$ K, a velocity $v \approx 20$ km s^{-1} with respect to the Sun [*Bertaux et al.*, 1985] and, in our models, by a density $n \approx 0.17$ cm^{-3} [*Ajello et al.*, 1994]. A recent tabulation of the rather wide range of hydrogen density values in the literature is given by *Puyoo, et al.* [1997]. Their work finds a neutral density at large distances of $n = 0.25 \pm 0.08$ cm^{-3}. Solar gravity acts to focus the hydrogen atoms as they pass the Sun, but is largely canceled by solar Lyman α radiation pressure that repels the atoms. The ratio of the radiation pressure to the solar gravity is called μ. Solar cycle variations in μ can make the Sun either repel the atoms or slightly focus them downstream. Fast moving solar wind protons charge exchange with the slower interstellar neutral hydrogen atoms, creating a population of fast moving hydrogen atoms Doppler-shifted outside the solar Lyman α line and leaving behind a cavity depleted in the slow neutrals that scatter solar Lyman α photons. Hydrogen atoms are also ionized by solar EUV radiation. Solar Lyman α resonance scattering from the surviving slow hydrogen atoms creates the observed glow.

Modeling the interplanetary Lyman α brightness pattern requires detailed understanding of the processes listed above. The Pioneer Venus Orbiter ultraviolet spectrometer (PVOUVS) interplanetary Lyman α observations provide a particularly good test of our understanding of the solar processes and their variations, since the data were obtained over more than a full solar cycle (December 29, 1978, to April 18, 1992) at a nearly constant distance of 0.72 AU from the Sun. Other spacecraft (Pioneer 10 and Voyagers 1 and 2) have obtained a long time series of interplanetary Lyman α observations, but these data sample a range of distances from the Sun, complicating the interpretation because of the possible presence of outer heliospheric effects [e.g., *Hall*, 1992; *Hall et al.*, 1993; *Quemerais et al.*, 1995, 1996]. Successful modeling of the PVOUVS inner heliosphere data set is a first step toward understanding the outer heliospheric data.

The modeling described here builds on our earlier efforts. *Ajello et al.* [1987] examined the PVOUVS interplanetary Lyman α data set (1979-1985) and used the parallax shift over the Venus year of the brightest emission region to determine the hydrogen atom lifetime. Ajello 1990 analyzed a unique set of PVOUVS Lyman α observations from 1986 covering high ecliptic latitudes during observations of Comet Halley. Improvements in the model reflect subsequent efforts at modeling Galileo and Voyager data described elsewhere [*Pryor et al.*, 1992, 1996; *Hall*, 1992; *Ajello et al.*, 1993, 1994]. This paper applies our latest models to the full PVOUVS data set. These models explicitly compute the solar Lyman α flux at each latitude and longitude as a function of time by using He 1083 nm images as a proxy for solar Lyman α [*Pryor et al.*, 1996].

[1]Laboratory for Atmospheric and Space Physics, University of Colorado, Boulder.
[2]Jet Propulsion Laboratory, Pasadena, California.
[3]High Altitude Observatory/National Center for Astmospheric Research, Boulder, Colorado.
[4]Federal Data Corporation/Jet Propulsion Laboratory, Pasadena, California.

Paper number 98JA01918.
0148-0227/98/98JA-01918$09.00

2. Instrumentation

The PVOUVS instrument [*Stewart*, 1980] was a compact 1/8-m Ebert-Fastie spectrometer with a programmable grating drive and two photomultiplier tube detectors. The Pioneer Venus Orbiter spin rate was typically 0.52 ± 0.01 rad s^{-1} before May 1981 and 0.48 ± 0.01 rad s^{-1} after that. The PV Orbiter spin axis was usually aligned within ~5° of the south ecliptic pole. The PVOUVS optical axis slanted 60° away from the spin axis. Thus the instrument field of view (1.4° x 0.14°) observed a small circular strip on the celestial sphere, with a 1.4° width, at an ecliptic latitude 30±5°S. The PVOUVS instrument sensitivity at Lyman α found in calibrations was 130 counts s^{-1} kR^{-1}. Observed stellar brightnesses indicate that the Lyman α sensitivity was nearly constant over the course of the mission.

3. Observations

The Pioneer Venus Orbiter maintained a polar orbit around Venus with a 24-hour period. Typical distances from planet center were ~70,000 km for apoapsis and 6200-8000 km for periapsis. Interplanetary Lyman α data were obtained at irregular intervals when ground stations were available and when Venus was not in conjunction with the Sun. The instrument operated in fixed grating position mode, typically using a 32-ms integration. This integration period leads to a spin smearing of about 0.9°. In orbits where two sets of 240° arcs were taken, the data were combined for a full 360° coverage in longitude. Figure 1 illustrates the spacecraft orbit and the PVOUVS observing geometry.

4. Data Reduction

Because PV obtained interplanetary Lyman α data near Venus, careful exclusion of the Lyman α signature of the Venus hydrogen corona was necessary. We examined the brightness of the corona as a function of the closest approach distance *d* of the look vector to the center of the planet [*Lasica et al.*, 1993]. Data obtained with *d* greater than 5 Venus radii from the planet center (30,255 km) had <5% contamination and could safely be included in the interplanetary data to be reduced. The coronal contamination was largest near solar maximum and was unobservable past 5 Venus radii at solar minimum. The Venus corona and its variation over a solar cycle are discussed by *Colwell* [1997]. A time-dependent instrumental background of 7-12 R due to cosmic rays was subtracted from the data. This background was largest near solar minimum and smallest near the two solar maxima.

Because of a minor problem in the grating drive system, different fixed grating positions were used to observe the Lyman α line during different parts of the mission. The reported intensities were corrected to reflect the part of the instrumental line profile being observed. No overall systematic offsets between data and model were identified that could be conclusively attributed to the use of these different grating steps. However, residual differences between data and models in early 1979 may be related to incompletely correcting for the transition from grating step 42 to step 41 on orbit 70 (1979 day 43).

5. Modeling

Plate 1 includes a color display of the PVOUVS data selected for modeling, with time on the horizontal axis and ecliptic longitude on the vertical axis. The data are brightest in upwind longitudes near ecliptic longitude 250° and dimmest near the downwind direction, where slow neutrals have been depleted by charge exchange and photoionization. Data became sparser as the mission progressed due to reduced ground station coverage. The brightest data are at the two ends of Plate 1 during maxima in the solar activity cycle. The data

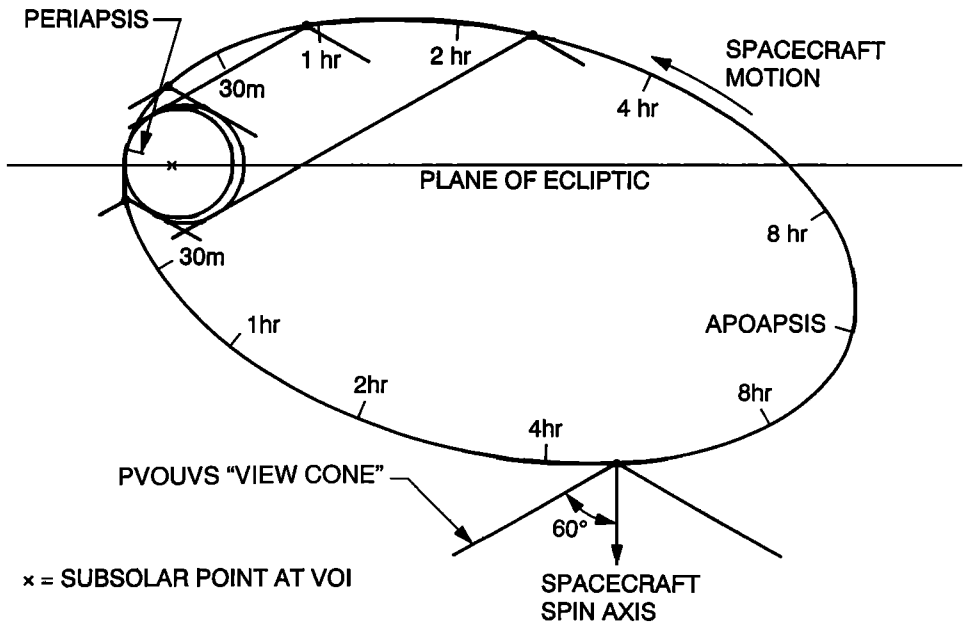

Figure 1. Illustration of the Pioneer Venus Orbiter polar 24-hour orbit. The PVOUVS observed in longitude circles at -30° ecliptic latitude. Interplanetary Lyman α data used here were obtained where the distance from the instrument look vector to the planet center exceeded 5 Venus radii. Times from periapsis are indicated. VOI stands for Venus Orbit Insertion.

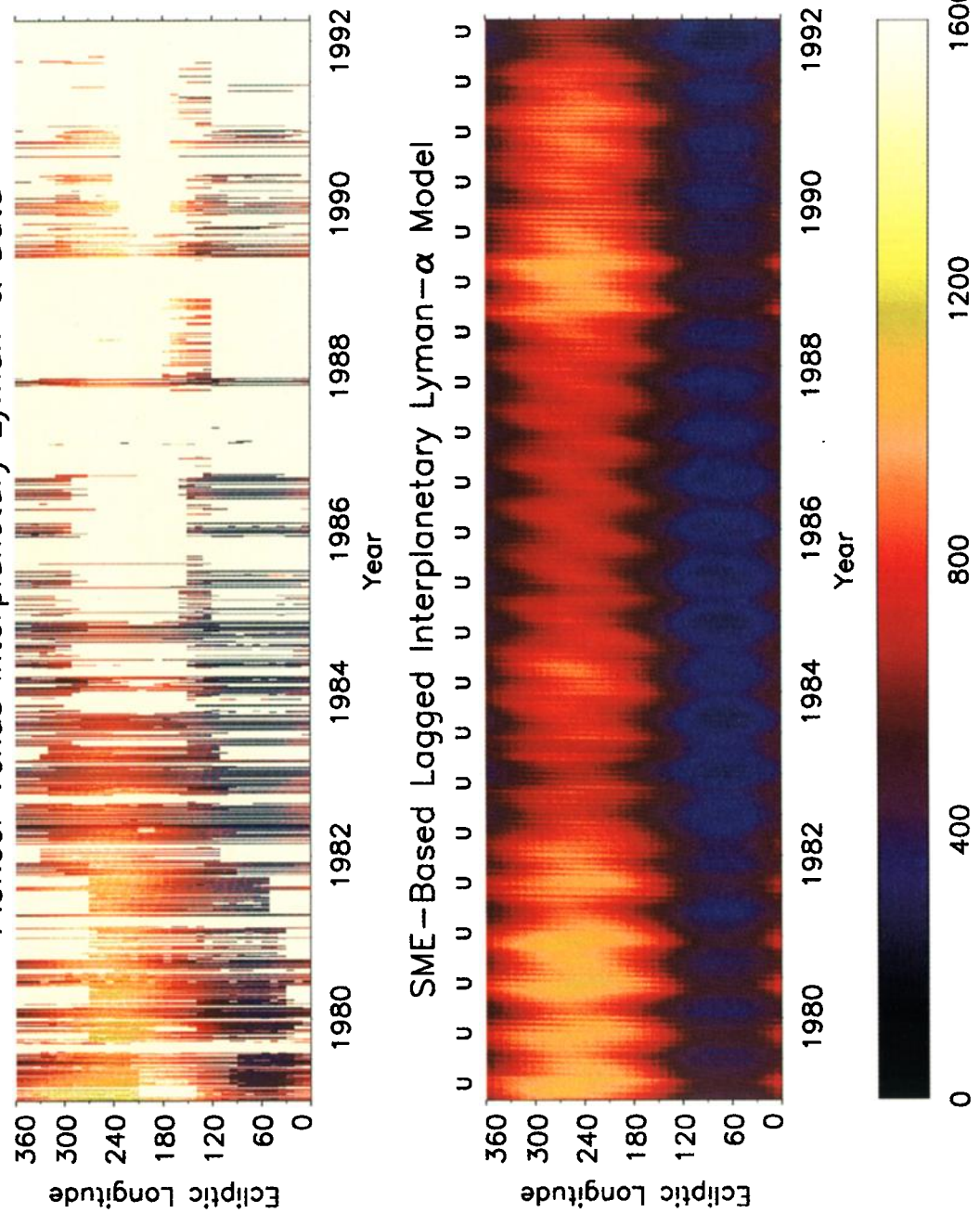

Plate 1. (a) The PVOUVS interplanetary Lyman α data selected for modeling as a function of time and ecliptic longitude. Bright colors represent the highest intensities, which occur in the upwind direction near ecliptic longitude 250°. Off white indicates no data. The top axis indicates Venus years: each U indicates when the spacecraft (and Venus) were both upwind. (b) The best fit SME-based "lagged" model (used in Plates 1 and 2 and Figures 6 and 7). The interstellar wind parameters were n=0.17 cm^{-3}, T=8000 K, and v=20 km s^{-1}. The solar wind asymmetry parameter was A=0.6. The solar flux, radiation pressure, hydrogen atom lifetime, and multiple scattering correction were varied in time as described in the text. Data and model were smoothed over three bins (30° in longitude) for clarity. The data elements have been widened by a factor of 4 because of printer limitations.

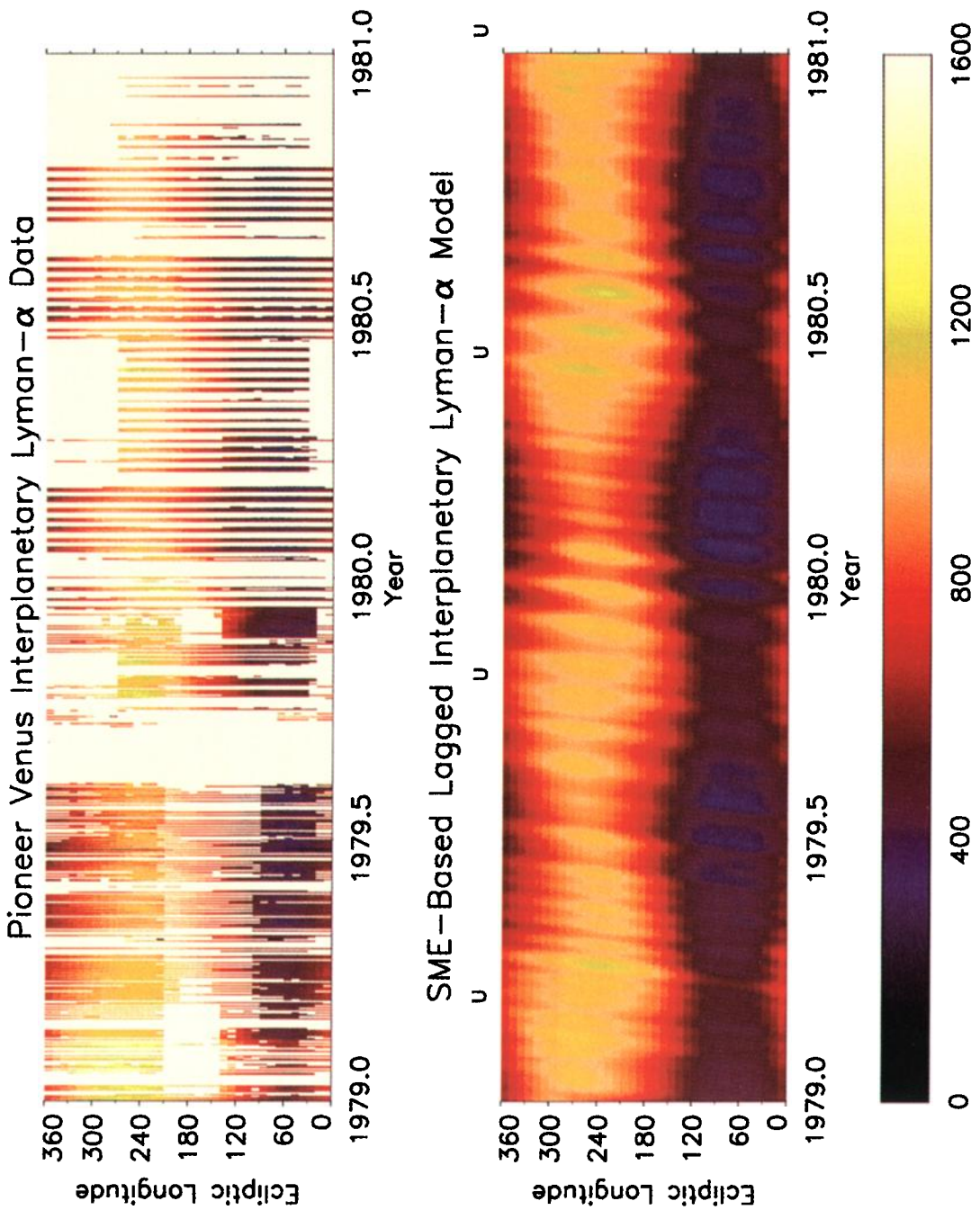

Plate 2. (a) The first 2 years of PVOUVS Lyman α data (1979-1981) selected for modeling, as a function of time and ecliptic longitude. Bright colors represent the highest intensities. Off-white indicates no data. The top axis indicates Venus years: each U indicates when the spacecraft (and Venus) were upwind. (b) the first 2 years of the best fit SME-based "lagged" model used in Plates 1 and 2 and Figures 6 and 7. Data and model were smoothed over three bins (30° in longitude) for clarity.

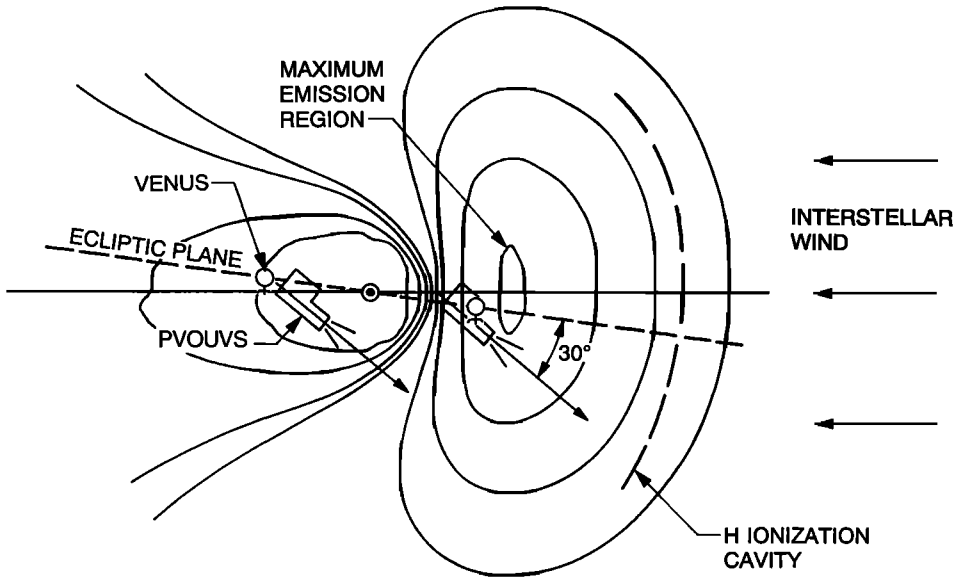

Figure 2. An illustration of the upwind-downwind viewing geometry at two spacecraft locations. The ecliptic plane is viewed edge-on. The interstellar wind (ISW) flows to the left. A cavity in the ISW hydrogen near the Sun is carved by solar wind protons charge exchanging with the slow interstellar neutral hydrogen population, creating fast neutrals which are Doppler-shifted off the solar Lyman α line and are therefore invisible. The contour lines schematically illustrate the variations in the Lyman α volume emission rate. It has a local minimum centered on the Sun, and a local maximum (the maximum emission region) upwind of the Sun, about halfway between the Sun and the upwind cavity boundary. Waves visible in Plates 1 and 2 related to the motion of Venus (and the PV Orbiter) about the Sun are due to distance variations between the look vector in the upwind direction and the maximum emission region. The PVOUVS views in longitude circles near -30° ecliptic latitude. These instrument look directions approach the maximum emission region more closely when the spacecraft is upwind.

taken from 1983 to 1987 are the least bright, corresponding to solar minimum.

The best fit SME-based "lagged" model is also presented in Plate 1. Details of this model will be discussed below. Plate 2 presents the data and best fit SME-based lagged model for the first 2 years of the mission. Apparent in the models (Plates 1b and 2b), and somewhat less apparent in the data, is a modulation or waviness in the upwind intensity associated with the 225-day orbital period of Venus. When the spacecraft is on the upwind side of the Sun (times marked with "U" in Plates 1a and 2a), it is closer to the upwind maximum emission region, increasing its angular extent (Figure 2). A parallax shift in the direction to the maximum emission region due to the orbital motion of Venus makes these waves appear diagonal in Figure 2. The brightness maximum on each wave tends to pass through the upwind direction when the spacecraft is directly upwind. In Plate 2 a diagonal variation is also visible correlated with the ~25-day sidereal rotation period (28 days as seen from Venus) of Lyman α bright solar active regions. A detailed study of one such wave was presented by *Ajello et al.* [1987].

The model developed for fitting Galileo extreme ultraviolet spectrometer data [*Pryor et al.*, 1996] was used here. This model is a version of a "hot" density model described by *Thomas* [1978]. The model has evolved to include latitudinal anisotropies in the solar wind flux [*Witt et al.*, 1979], as well as latitudinal and longitudinal anisotropies in the solar Lyman α flux [*Pryor et al.*, 1992, 1996]. One troubling, persistent problem found in our modeling efforts is the difference in absolute calibrations at Lyman α between different spacecraft. PVOUVS reported Lyman α intensities are ~2.13 times lower than simultaneous measurements by Galileo when it passed Venus [*Colwell* 1997; also personal communication 1998]. Throughout this paper, the PVOUVS values are scaled to the Galileo-based model values. The scaling factors are near 2 but vary somewhat due to modeling variations and uncertainties. Using the Galileo calibration [*Hord et al.*, 1992], the current models require a high number density of hydrogen inside the termination shock, n=0.17 cm^{-3} [*Ajello et al.*, 1994] as opposed to earlier models that found n=0.07±0.01 cm^{-3} [*Ajello et al.*, 1987], somewhat increasing the importance of multiple scattering.

We prefer to use the more recent Galileo calibration for the following reasons. Because of launch delays, there was adequate time for extensive characterization and calibration of the Galileo UVS. The Galileo UVS laboratory absolute calibration at wavelengths greater than 1300 Å, based on National Institute of Standards and Technology (NIST) standard photodiodes, is estimated to be accurate to better than 20%. We also obtained Galileo UVS laboratory spectra of electron impact on H_2 and N_2 that provide a high-quality relative calibration in the FUV, including Lyman α [*Ajello et al.*, 1988; *Hord et al.*, 1992]. The estimated additional uncertainty at Lyman α with this technique is ~20%. Comparison of Galileo UVS spectra of the star Sirius with rocket observations shows excellent agreement (<20%) at wavelengths greater than 1300 Å where sufficient stellar signal is present (W. McClintock, private communication, 1998]. Based on these considerations, the density derived from Galileo Lyman α measurements, including estimated error bars from the calibration only, is ~0.17 ± 0.05 cm^{-3}.

The density used here should also be compared to neutral hydrogen density estimates from pickup ion studies. *Gloeckler et al.* [1997] used Ulysses solar wind ion composition spectrometer (SWICS) pickup ion measurements to derive a neutral hydrogen density near the termination shock of 0.115

± 0.025 cm^{-3}. The SWICS estimate and the Galileo estimate have overlapping error bars. Another technique, measurement of the solar wind slowdown due to mass loading, has been studied by *Richardson et al.* [1995]. From a measured solar wind slowdown of ~30 km s^{-1} between 1 and 40 AU, they estimate a low neutral hydrogen density of 0.05 cm^{-3}, based on theory presented by *Lee* [1997]. Another model for the slowdown presented by *Isenberg* [1986, Figure 2] shows that a slowdown of ~30 km s^{-1} at 40 AU corresponds to a neutral hydrogen density of 0.1 cm^{-3}, closer to the *Gloeckler et al.* results. Recent work by *Isenberg* [1997] shows that a neutral hydrogen density of 0.125 cm^{-3} near the termination shock is consistent with an analysis of anomalous cosmic ray spectra by *Stone et al.* [1996].

The solar cycle variations of five quantities are included in the model as follows:

5.1. Solar Flux Variation

Our model uses solar He 1083-nm images to compute the solar Lyman α flux on a given day at any solar latitude and longitude [*Pryor et al.*, 1996]. The He 1083-nm image set obtained at Kitt Peak provides a valuable indicator of the Sun's Lyman α distribution. The disc-averaged equivalent width is an excellent proxy for Lyman α [*Harvey*, 1984; *Tobiska* 1991; *Harvey and Livingston*, 1994]. Harvey and colleagues have combined these images into Carrington rotation maps, which provide the equivalent width as a function of latitude and longitude for each solar rotation. These Carrington maps form the basis for our calculation. First, holes and artifacts in these images were corrected by using information from neighboring Carrington rotations. This procedure may introduce some errors in the record, particularly in the late 1970s when more data gaps were present. Next, an integral was performed which finds the disc-averaged equivalent width that would be seen above any solar latitude and longitude on any given day. This procedure reproduces in considerable detail the previously reported disc-integrated equivalent widths in the ecliptic plane. It was then assumed that the same linear relationship that exists between the ecliptic plane disc-averaged equivalent width of He 1083-nm and disc-integrated, line-integrated Lyman α flux [*Tobiska*, 1991] exists at all other latitudes. Two different relationships were used here. The linear relationship between the He 1083-nm equivalent width (EW) and the Solar Mesosphere Explorer (SME) line-integrated solar Lyman α measurements is [*Tobiska*, 1991]

$$\text{Lyman } \alpha \text{ SME} = 8.40\times10^{10} + 3.78\times10^{9}\times\text{EW}$$

in units of photons cm^{-2} s^{-1} at 1 AU from the Sun. Measured values of EW range from 39 to 97. The linear relationship between the He 1083 nm equivalent width and the Upper Atmosphere Research Satellite (UARS) solar Lyman α time series in the same units (through the end of 1995) is

$$\text{Lyman } \alpha \text{ UARS} = 0.95\times(2.10\times10^{10}+7.07\times10^{9}\times \text{EW}).$$

The UARS data come from the Solar Stellar Intercomparison Experiment (SOLSTICE) measurements [*Woods and Rottman*, 1997] and have been scaled by the factor of 0.95 because the other Lyman α instrument on UARS (Solar Ultraviolet Spectral Irradiance Monitor (SUSIM)) reports Lyman α values 10% lower than SOLSTICE. The UARS instruments were probably better calibrated than SME. The relative calibration as a function of time of SOLSTICE is closely monitored by measurements of a suite of stars. The UARS Lyman α fluxes are systematically higher than the SME measurements, by ~30% or more, and have a larger solar maximum to solar minimum ratio [*Woods and Rottman*, 1997; *Tobiska et al.*, 1997; *de Toma et al.*, 1997]. Figure 3a shows the computed ecliptic and polar Lyman α fluxes for the SME model. As we have previously suggested [*Pryor et al.*, 1992; *Ajello et al.*, 1994], the computed polar Lyman α flux is substantially (~20%) below the equatorial flux at solar maxima. Figure 3b compares the SME-based and UARS-based ecliptic Lyman α fluxes.

A key assumption in the modeling is that the unmeasured Lyman α line center flux (photons cm^{-2} s^{-1} $Å^{-1}$) responsible for resonance scattering from interstellar neutral hydrogen equals about 0.9 $Å^{-1}$ times the SME- or UARS-derived integrated solar Lyman α flux (photons cm^{-2} s^{-1}) throughout the solar cycle. *Ajello et al.* [1987] used PVOUVS data to show that this ratio is fairly constant over the solar cycle. The rough validity of this assumption is tested here by trying models that assume the factor of 0.9 $Å^{-1}$ for all orbits. The 0.9 $Å^{-1}$ estimate comes from recent measurements of the disc-integrated solar Lyman α line shape obtained at solar minimum by the Solar Ultraviolet Measurements of Emitted Radiation (SUMER) instrument on the Solar Heliospheric Observatory (SOHO) [*Lemaire et al.*, 1998]. Our previous models [*Ajello et al.*, 1987, 1994; *Pryor et al.*, 1992, 1996] assumed a factor of 1.0 $Å^{-1}$. SUMER results from closer to solar maximum may shed light on this problem in the future.

5.2. Solar Radiation Pressure Variation

Estimates of the radiation parameter μ also rely on assuming the numerical correspondence between line center and integrated solar Lyman α emissions. The radiation pressure has a latitude dependence directly caused by the latitude dependence of the solar flux [*Ajello et al.*, 1994]. Atoms that pass over the solar poles are exposed to a lower average radiation pressure than those that pass over more equatorial latitudes. This effect is crudely represented by averaging the 12-month average ecliptic value of μ, with the lower polar value. The time average is used to compensate for the varying pressures experienced by a hydrogen atom as it approaches and then recedes from the Sun. During a 1-year period a hydrogen atom travels 4.2 AU at a velocity of 20 km s^{-1}. This is roughly comparable to the scale size of the system: the maximum emission region is at distances $r_c/2$ from 2.25 to 3.35 AU from the Sun, depending on the hydrogen atom lifetime [*Ajello et al.*, 1987]. Here r_c is the distance along the upwind axis from the Sun to the point where ionization has attenuated the original density by a factor of $1/e$.

Both the ecliptic value and polar values of μ are estimated from the He 1083-nm solar images. The solar flux information in Figures 3a and 3b is used to compute the equatorial and polar 1-year-average ratio of radiation pressure to solar gravity. The computed polar 1-year-average radiation pressure is lower than the equatorial value by 10-20% at solar maxima. For modeling purposes we use the average of the polar and equatorial 1-year-average radiation pressures, shown in Figure 3c. SME and UARS-based models of the radiation pressure are both shown for cases with the line center flux equal to 0.9 $Å^{-1}$ and 1.0 $Å^{-1}$ times the line-integrated flux. The radiation pressure parameter μ for the SME-based Lyman α fluxes is gener-

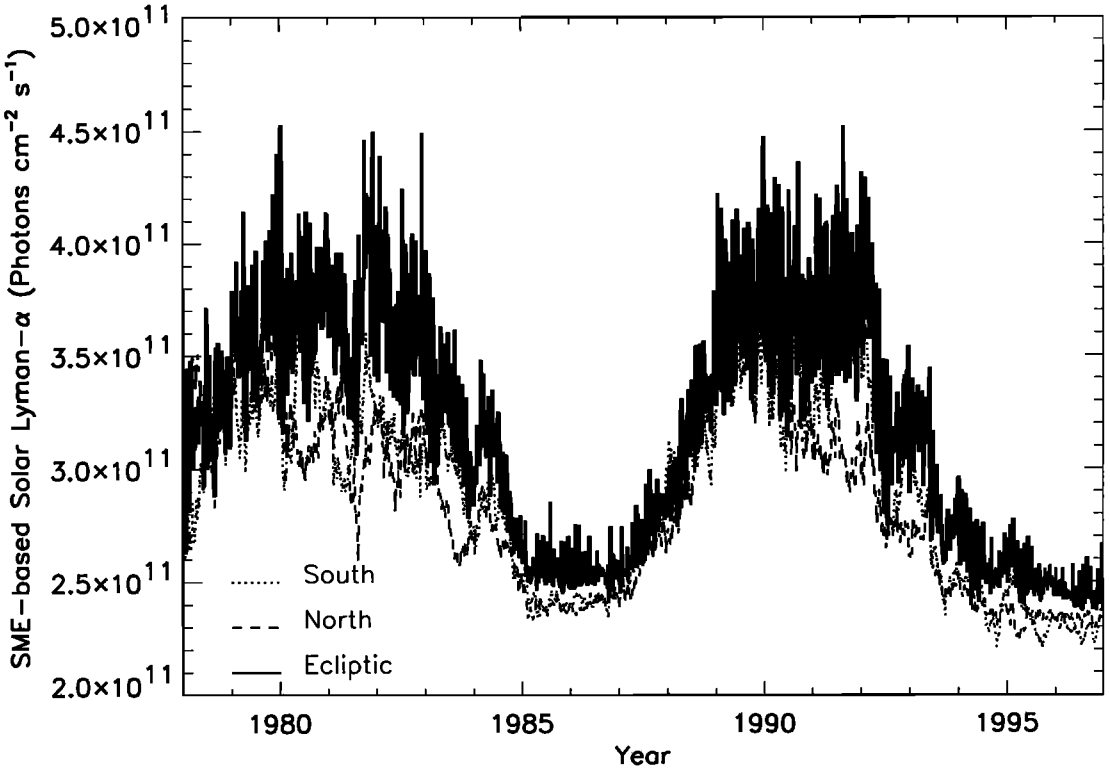

Figure 3a. The daily SME-based solar Lyman α line-integrated flux for the ecliptic plane and for the two solar poles for the PV period. Values are taken from the He 1083-nm calculation using the proxy model described in the text. Models in this paper use the line center flux, assumed to be 0.9 times the values shown.

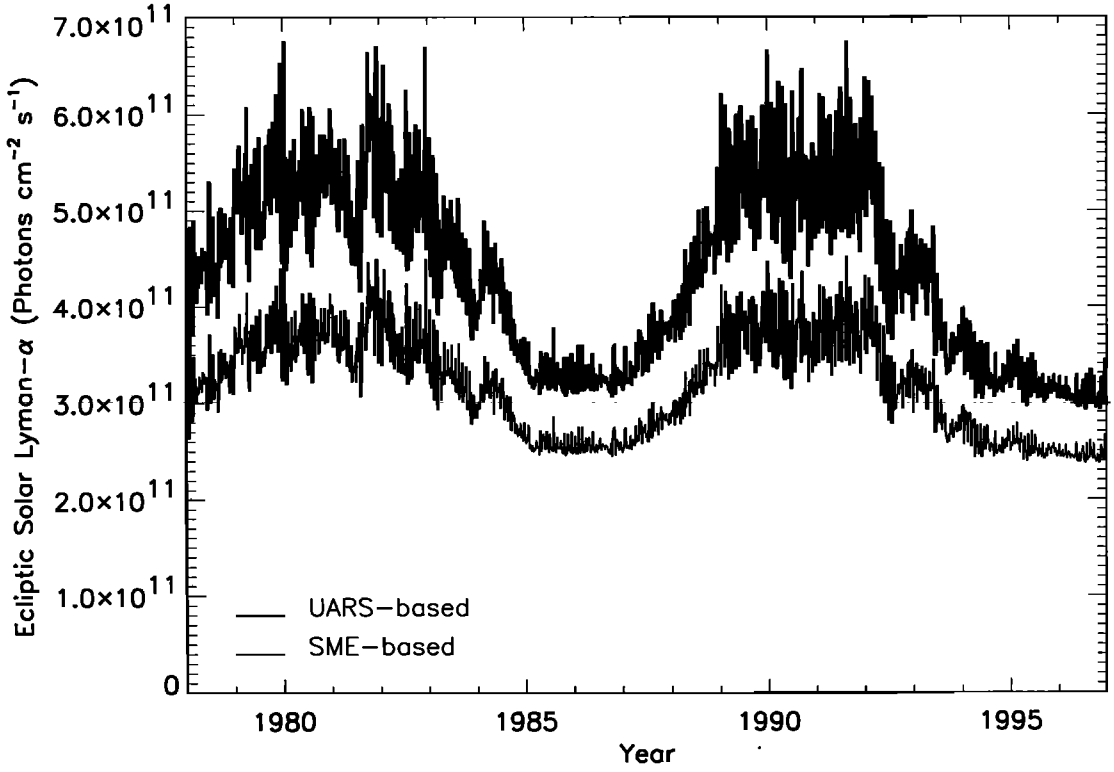

Figure 3b. The SME- and UARS-based solar Lyman α line-integrated ecliptic flux computed from the He 1083-nm calculation. Models in this paper use the line center flux, assumed to be 0.9 times the values shown.

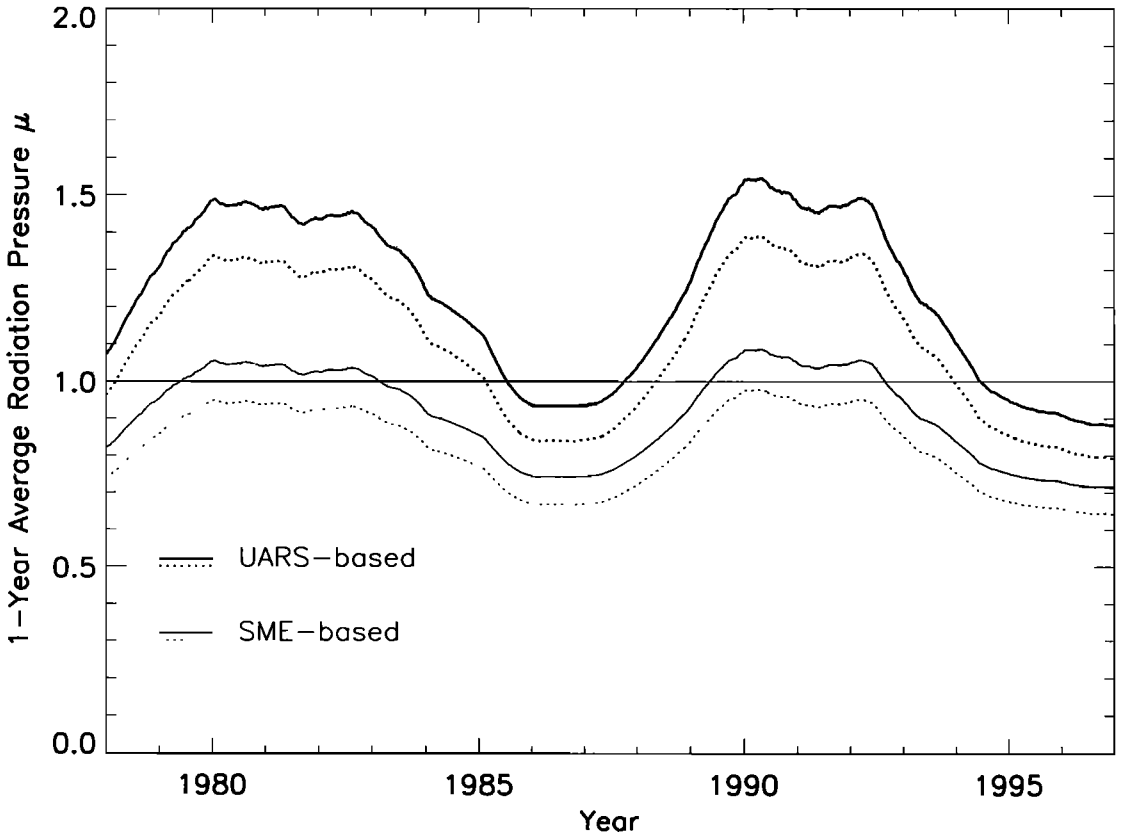

Figure 3c. Assuming a one-to-one correspondence between the numerical values of line-integrated Lyman α solar flux (photons cm^{-2} s^{-1}) and line center Lyman α solar flux (photons cm^{-2} s^{-1} $Å^{-1}$) leads to 1-year average (before the indicated date) radiation pressure parameter μ values for SME and UARS fluxes. The average of the north and south polar μ values has been averaged with the ecliptic μ value to estimate the "average" radiation pressure (solid lines). Models in this paper use radiation pressure values (dashed lines) equal to 0.9 times the solid lines. The horizontal line at μ=1 separates μ values that lead to a net solar attraction of hydrogen atoms by the sun (μ<1) from values with net solar repulsion (μ>1).

ally less than 1, so the net effect in passing the Sun is focusing. However, the UARS-based Lyman α fluxes imply μ generally >1, so the net effect is repulsion.

5.3. Solar Wind Flux Variation

Charge exchange between slow (20 km s^{-1}) interstellar hydrogen atoms and faster (~300-700 km s^{-1}) solar wind protons creates a cavity near the Sun depleted in slow neutrals that can scatter the solar Lyman α line. The rate of this process in the ecliptic is estimated from the National Space Science Data Center (NSSDC) on-line database of solar wind proton density and velocity measurements at 1 AU. These measurements made by the near-Earth spacecraft ISEE 1, ISEE 3, IMP 7, and IMP 8 are documented by *King* [1977a, b, 1979, 1983]. Most of the data used here come from the IMP 8 spacecraft. Hydrogen atom-proton charge exchange cross sections are from *Barnett et al.* [1990]. The rate of the charge exchange process at other ecliptic latitudes is not well known; finding this rate is one goal of our modeling efforts. If τ(0) is defined to be the time-averaged lifetime against solar wind charge exchange in the ecliptic (ecliptic latitude 0 degrees), then the lifetime at ecliptic latitude β is assumed to be of the form

$$\tau(\beta)=\tau(0)/[1. - A \sin^2(\beta)]$$

where A is the solar wind asymmetry parameter.

Our initial model approximates the varying solar wind fluxes encountered by the interstellar neutrals by averaging the solar wind flux over the 12 months before a given observation. This is the same timescale used for the radiation pressure calculation, for the same reasons discussed above. Figure 4 shows the monthly average hydrogen lifetime against solar wind charge exchange at 1 AU and the 12-month-average lifetime. The average values range from ~1.2 to 1.9×10^6 s. The actual lifetime will be somewhat shorter due to solar EUV photoionization of hydrogen.

5.4. Solar EUV Flux Variation

A secondary loss process for ground state (1s) interstellar hydrogen is photoionization by photons with wavelengths less than 91.2 nm. The solar EUV flux variation over a solar cycle is not particularly well known. *Ogawa et al.*, [1995] evaluated the total photoionization rate β, including a very minor component from loss of metastable (2s) hydrogen. Using *Ogawa et al.'s*, Table 3, we represent the total photoionization rate at 1 AU, β, in s^{-1} as

$$\beta = 1.50 \times 10^{-7} + (2.42 \times 10^{-7} - 1.50 \times 10^{-7})$$

$$\times ((F10.7-62.7)/(214.0-62.7))$$

where F10.7 is the 10.7 cm radio flux from the Sun in units of 10^{-22} W m^{-2} Hz^{-1}. The photoionization lifetime τ is the recip-

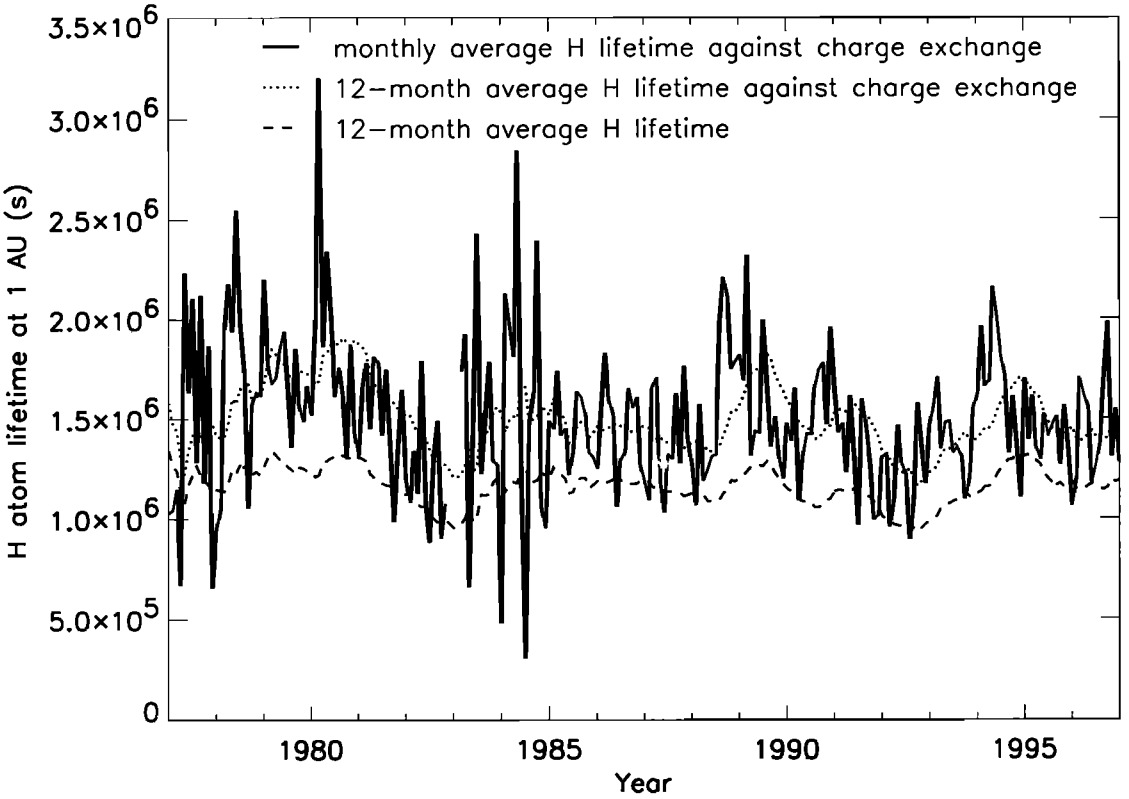

Figure 4. The variation in the monthly average hydrogen atom lifetime against solar wind charge exchange. Also shown is the 12-month average of the monthly average lifetime before a given time, for charge exchange only; and for charge exchange combined with photoionization. Values of solar wind density and velocity are taken from the National Space Science Data Center (NSSDC) database.

rocal of β. A value of F10.7=62.7 is a very low solar minimum value, while F10.7=214.0 is more typical of solar maximum conditions. For a solar minimum value of F10.7=62.7, $\beta=1.50\times10^{-7}$ s^{-1} and $\tau=6.67\times10^{6}$ s. For a solar maximum value of F10.7=214.0, $\beta=2.42\times10^{-7}$ s^{-1} and $\tau=4.13\times10^{6}$ s. In both cases the photoionization lifetime τ is substantially longer than the hydrogen atom lifetime against solar wind charge exchange. One-year averages of the photoionization lifetime were used in the models here. Combining the photoionization lifetime and the solar wind charge exchange lifetime yields a surprisingly constant lifetime for slow neutral hydrogen (Figure 4). Photoionization is largest near solar maximum when the charge exchange rate is smallest. The ecliptic lifetime found from solar wind and solar EUV flux measurements in Figure 4 is generally near ~1.2×10^{6} s. This compares favorably with the lifetime of 1.1×10^{6} sec derived from parallax shifts of the maximum emission region in Pioneer Venus interplanetary data [*Ajello et al.*, 1987].

5.5. Multiple Scattering Correction

Next, the time dependence of the multiple scattering correction was included in our optically thin model. (Current computational limits favor a hybrid approach between fast optically thin models and slow multiple scattering codes.) The multiple scattering model used [*Hall*, 1992; *Ajello et al.*, 1994] assumes cylindrical symmetry; no attempt is made to deal with latitudinal variations in the solar wind flux or the solar Lyman α flux. Multiple scattering corrections were computed for six cases, involving three realistic values of the radiation pressure and two values of the hydrogen atom lifetime at 1 AU. Linear interpolation between these six cases was made to derive the multiple scattering corrections appropriate for a given day. These corrections were computed for a spacecraft 1 AU downstream from the Sun, with values for atomic H outside the cavity but well inside the heliopause, of n=0.17 cm^{-3}, v=20.0 km s^{-1}, and T=8000 K. The dependence on distance from the sun and on spacecraft ecliptic longitude is assumed to be minor. The corrections to an optically thin model brightness I_{thin} are represented as

$$I(\theta)=I_{thin}(\theta)q(\theta)$$

The angle from the upwind direction is denoted θ. For θ=0, upwind, the corrections are negligible (<2%), while downstream, θ=180, they become important. The monotonically increasing function $q(\theta)$, where θ is in degrees, can be well represented as a polynomial:

$$q(\theta)=a_0+a_1\,\theta+a_2\,\theta^2+a_3\,\theta^3$$

Table 1 shows the six cases used. This multiple scattering correction scheme was used for all models shown. A similar calculation for n=0.10 cm^{-3} gave similar results (within 3%), indicating that the correction factors are not a strong function of density between 0.10 and 0.17 cm^{-3}. An independent calculation by *Quemerais and Bertaux* [1993, Table 3] found that q increases from 1.09 to 1.23 to 1.30 to 1.34 to 1.36 in the downwind multiple scattering correction when the density

Table 1. Multiple Scattering Corrections

τ, s	μ	a_0	a_1	a_2	a_3	$q(180)$
1.4x10⁶	0.75	0.99129	-2.1501x10⁻⁴	6.0459x10⁻⁶	2.6745x10⁻⁸	1.301
1.4x10⁶	1.10	0.98381	8.1145x10⁻⁵	-2.6860x10⁻⁶	9.5069x10⁻⁸	1.462
1.4x10⁶	1.60	0.97097	6.0193x10⁻⁴	-1.8731x10⁻⁵	2.1399x10⁻⁷	1.716
2.1x10⁶	0.75	1.0005	-3.1373x10⁻⁴	7.8907x10⁻⁶	-4.1819x10⁻¹⁰	1.195
2.1x10⁶	1.10	0.99048	1.7690x10⁻⁵	-8.1105x10⁻⁷	7.06844x10⁻⁸	1.377
2.1x10⁶	1.60	0.97638	4.8491x10⁻⁴	-1.7107x10⁻⁵	1.9652x10⁻⁷	1.651

(n=0.17 cm^{-3})

increases from 0.01 to 0.05 to 0.1 to 0.15 to 0.20 cm^{-3}, for an observer 1 AU from the Sun and 90° from the upwind axis. Their results support the idea that the multiple scattering correction is not too sensitive to density variations in the range 0.1-0.2 cm^{-3}.

Increasing radiation pressure depletes the downwind density, leading to a very anisotropic density distribution. Multiple scattering produces a brightness distribution that is less anisotropic than would be obtained in a single-scattering model. The derived multiple scattering corrections are a strong function of the assumed radiation pressure. A hydrogen atom lifetime at 1 AU of 1.4x10^6 s is fairly realistic; changing to a 50% longer and less realistic lifetime of 2.1x10^6 s has only a modest effect on the correction. An extensive discussion of these radiative transfer effects is presented by *Quemerais and Bertaux* [1993].

6. Modeling Results

An initial attempt was made to fit the time series of the upwind and downwind data sets with an SME-based model, where the radiation pressure, hydrogen atom lifetime, and mul-

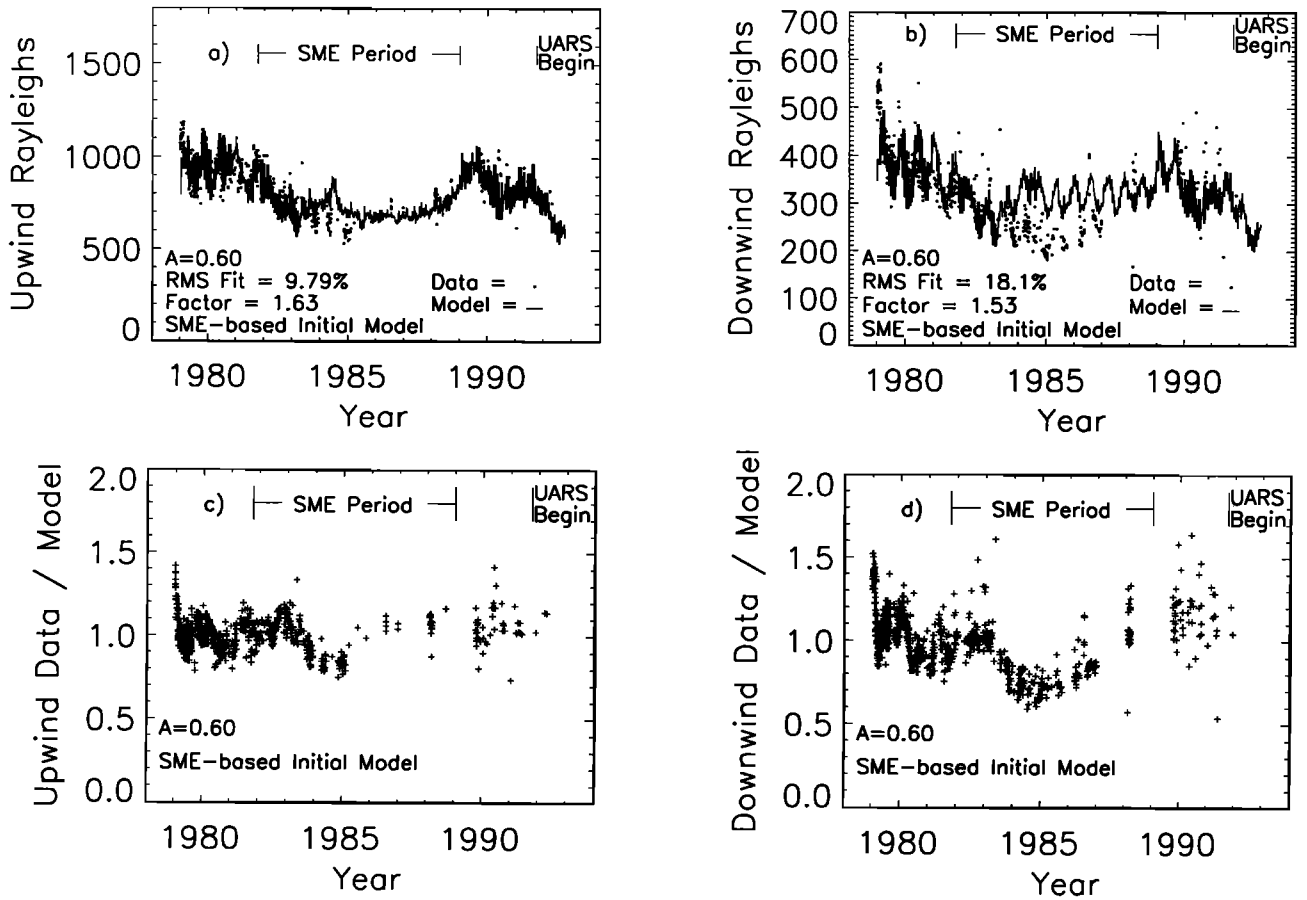

Figure 5. Initial model fits to the time series PVOUVS interplanetary Lyman α data. The data have been scaled upward to fit the model derived for Galileo data of *Pryor et al.*, [1996]. This scaling reflects calibration differences between instruments. This initial model uses solar radiation pressure, solar wind ionization, and photoionization values averaged over the 1 year prior to the observation. A solar wind asymmetry parameter of A=0.6 was used. (a) Fit to the upwind data. Data represent the average of three 10° bins centered on the upwind direction. Model points have been computed for each day and connected with a line for clarity; data are shown as dots, the actual locations of points can be more easily seen in Figures 5c and 5d. (b) Fit to the downwind data with the same model. Data represent the average of six 10° bins centered on the downwind direction. This model fits the downwind time series poorly. (c) The time series of data divided by model in the upwind direction. (d) The time series of data divided by model in the downwind direction.

tiple scattering correction are all represented as a 1-year average before the time of the observation. The upwind and downwind time series data with the Pioneer Venus calibration are independently scaled to the Galileo-based model. For successful models the two scaling factors should be similar and near 2 in order to match the cross-calibration results obtained when both PV and Galileo were near Venus. A solar wind asymmetry factor of A=0.6 was used (Figures 5a-5d). Three bins 10° wide in ecliptic longitude centered on the upwind direction were modeled separately and then combined to form the upwind set. Six of the dimmer 10° bins centered around downwind were combined to provide counting statistics similar to those of the upwind set. The downwind bin containing the star Iota Orionis was excluded. Each data point in this set contains at least 85 counts, while most contain several hundred counts. The upwind data are in fair agreement with the model, but the downwind data lead to a systematic problem: the data are higher than the model near the two solar maxima and lower than the model near the solar minimum.

Physically, the light observed downwind is coming from hydrogen atoms which passed the sun in earlier years (see Appendix A for more justification). This travel time effect suggests that the 1-year-averaging scheme is not adequate for describing the downwind hydrogen. Hydrogen atoms downwind at solar minimum may have passed the Sun at solar maximum, when the radiation pressure is much larger. A variation on the model was constructed to account for the time lag. Upwind volume emission rates are computed using the radiation pressure and hydrogen atom lifetimes averaged over 1 year before the observation. For downwind volume elements the radiation pressure and hydrogen atom lifetimes are averaged over 1 year before the time when the atoms in that volume element cross a plane 6 months downwind of the Sun, assuming a bulk hydrogen velocity of 20 km s^{-1}. This approximation assumes that the largest effect on the atoms occurs in the year when they are closest to the sun (Appendix A). Solar wind 1-year-average ecliptic data were used beginning in January 1975. Radiation pressure 1-year-average data derived from He

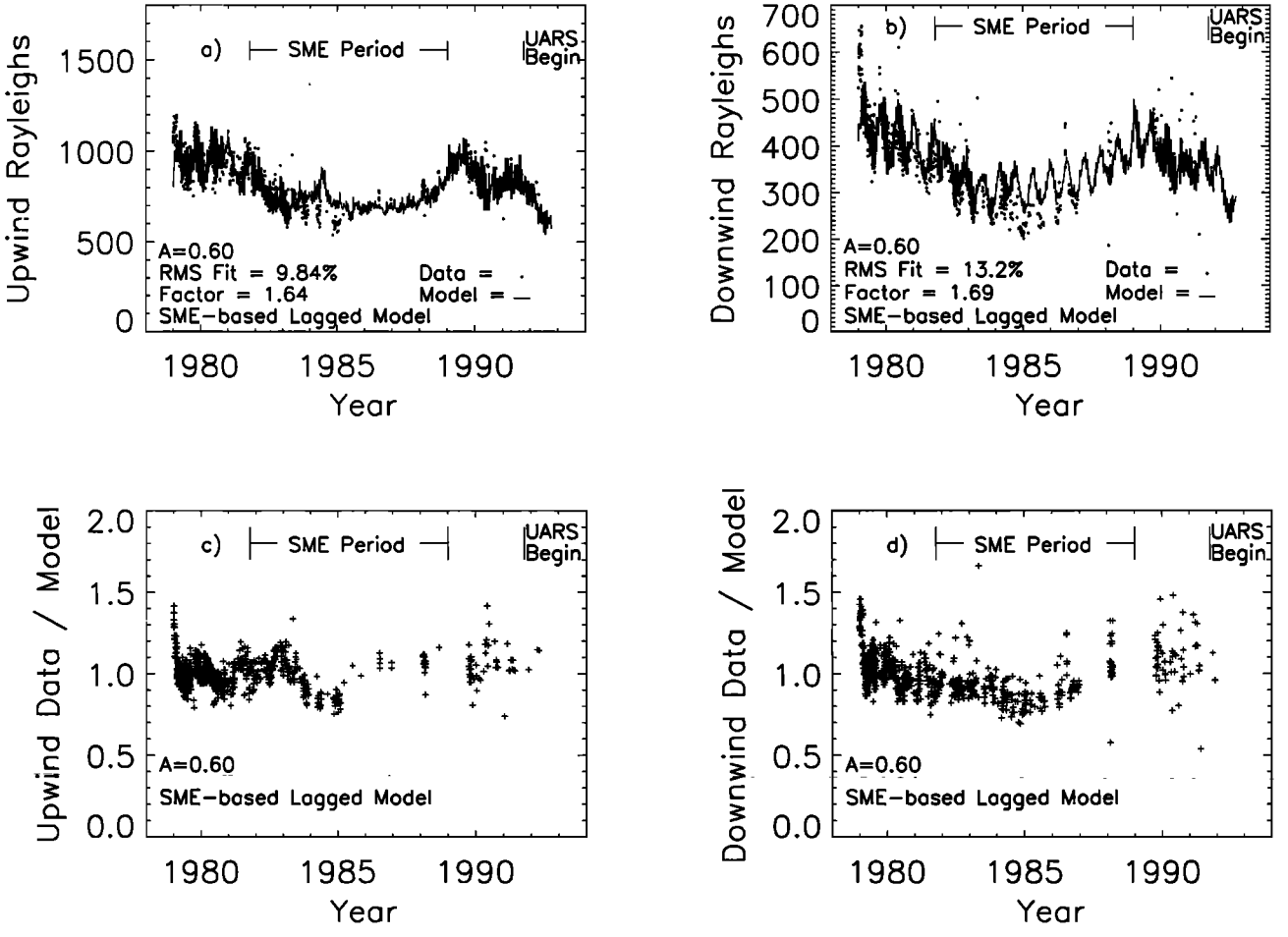

Figure 6. The fit of the best SME-based lagged model (used in Plates 1 and 2 and Figures 6 and 7) to the time series PVOUVS interplanetary Lyman α data. This model computes downwind densities using solar radiation pressure and solar wind ionization and photoionization values averaged over the year when the downwind hydrogen atoms had crossed the upwind-downwind plane, assuming a bulk downwind flow of 20 km s^{-1}. Upwind densities are computed for radiation pressure and ionization values averaged over 1 year before the observation. Scaling factors have been applied to the data with the PV calibration to bring them into agreement with the Galileo-derived model. A solar wind asymmetry parameter of A=0.6 was used. (a) Fit to the upwind data. Data (points) represent the average of three 10° bins centered on the upwind direction. (b) Fit to the downwind data with the same model. Data (points) represent the average of six 10° bins centered on the downwind direction. This model does better at fitting the downwind time series than the model in Figure 5. (c) The time series of data divided by model in the upwind direction. (d) The time series of data divided by model in the downwind direction.

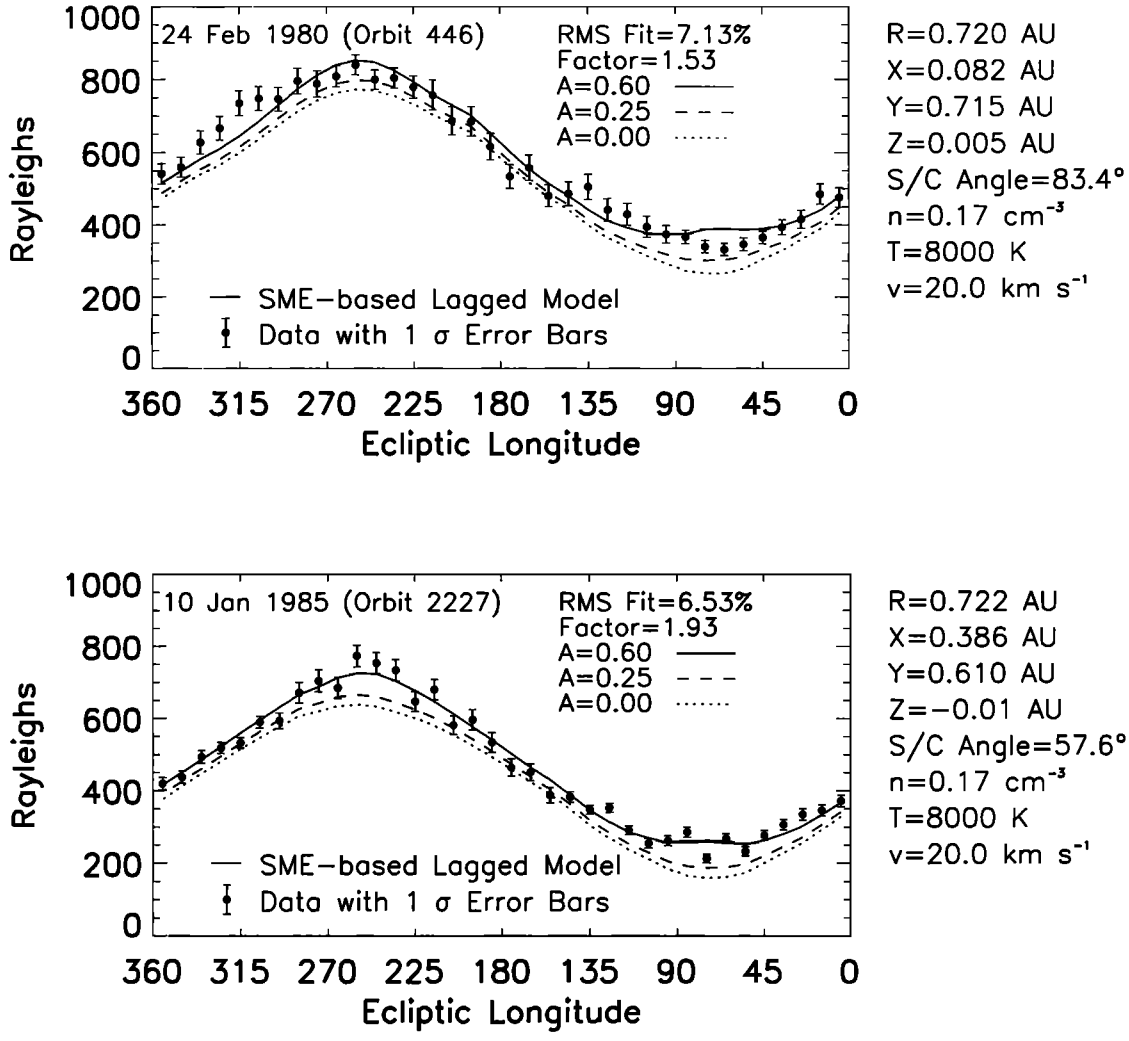

Figure 7. The fit of the best (A=0.6) SME-based lagged model (used in Plates 1 and 2 and Figures 6 and 7) to PVOUVS interplanetary Lyman α data from two "typical" days. Scaling factors have been applied to the data to bring them into agreement with the solar wind asymmetry parameter A=0.6 model. Also shown are models with A=0.25 and A=0.0. (a) For February 24, 1980 (orbit 446), during solar maximum. (b) For January 10, 1985 (orbit 2227), during solar minimum.

1083 nm images was used beginining in July 1977. The values for January 1975 and July 1977 were used for the solar wind and radiation pressure data, respectively, when examining volume elements where the atoms had passed the Sun before those two dates. As our PV data span 1979-1992, this is not a major handicap in the modeling, except possibly in the first year or two. Figures 6a-6d show the results of this SME-based lagged model. The quality of the downwind fit to the data is now much closer to the quality of the upwind fit, suggesting that this crude time-dependent model has captured the essence of the effect. This lagged model also fits the upwind-downwind variation observed on individual daily data sets. This is illustrated in Figure 7 for two "typical" days, one near solar maximum and one near solar minimum. Figure 7 also illustrates the effect of the solar wind asymmetry parameter A on the upwind to downwind ratio. Increasing A reduces this ratio, although we should again point out that many factors influence the upwind to downwind ratio and that the PVOUVS data are not ideal for determining A.

Finally, we show a lagged model based on the UARS SOLSTICE solar fluxes, which are systematically higher than the SME fluxes, and have a larger solar maximum to solar minimum brightness ratio. *Woods and Rottman* [1997] suggest scaling the UARS SOLSTICE fluxes by 0.95 to reflect the average of the UARS SOLSTICE and UARS SUSIM Lyman α measurements. This is done here for both the model solar Lyman α flux and the model radiation pressure. This model handles the time dependence in the same way as in Figure 6. Figures 8a-8d show the UARS-based fit to the time series, in this case for A=0.75. The model brightnesses are not very different from before because increasing the radiation pressure has largely compensated for the increasing solar flux. The downwind time series data are now better fit by the model. The large radiation pressure associated with the UARS fluxes depletes the downwind hydrogen more than in an SME-based model. For a UARS-based model with A=0.5 the scaling factors upwind and downwind are ~20% different, with an upwind scaling factor to apply to the data of 1.99 and a downwind factor of 1.65. Using A=0.75 provides somewhat better agreement (within ~10%) in scaling factors: upwind is 2.03 and downwind is 1.82. This asymmetry parameter corresponds to a polar hydrogen atom lifetime 4 times longer than the equatorial one.

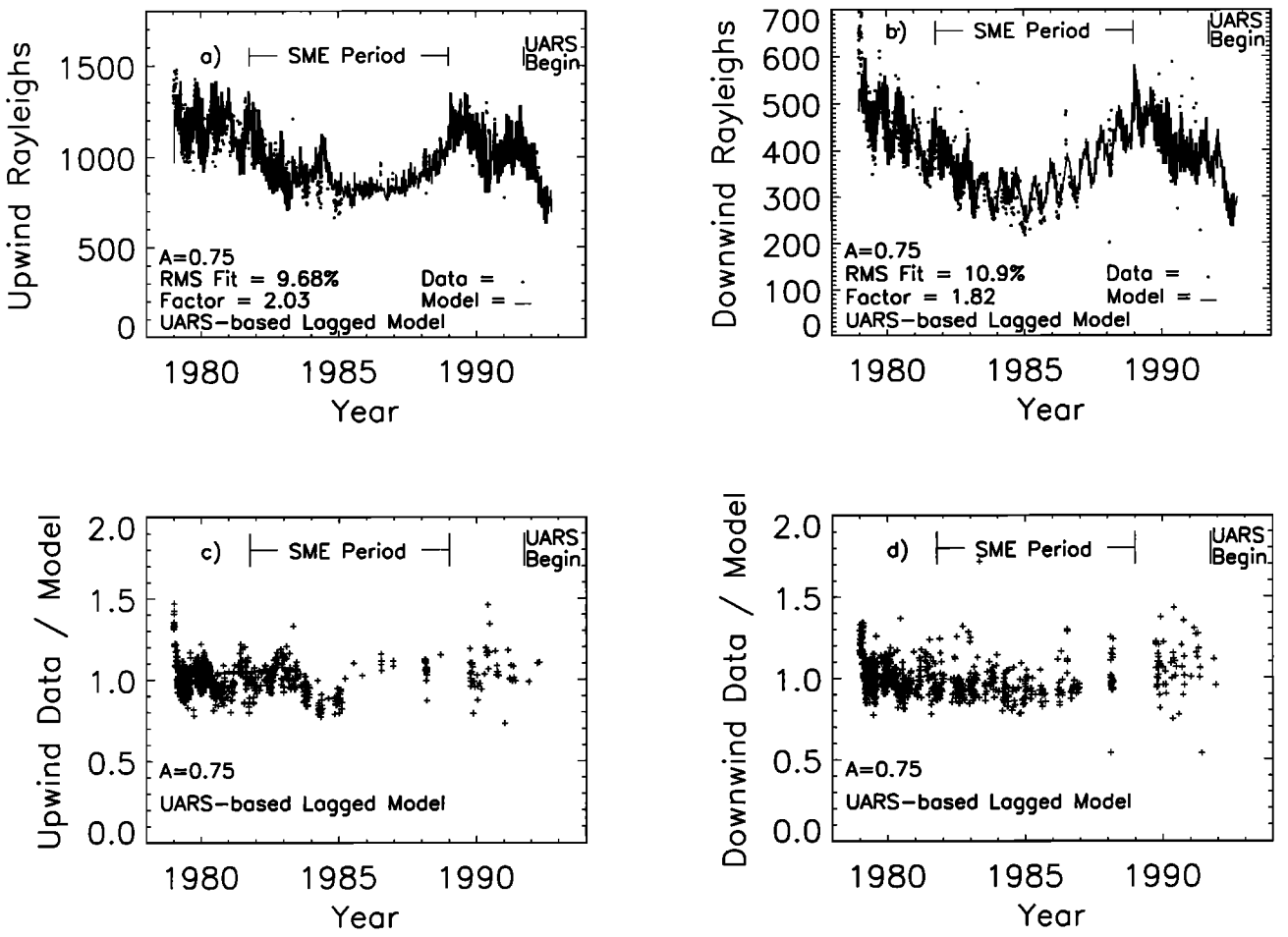

Figure 8. The fit of a UARS-based lagged model (solid line) to the time series PVOUVS interplanetary Lyman α data. This model computes downwind densities using solar radiation pressure and solar wind ionization and photoionization values averaged over the year when the downwind hydrogen atoms had crossed the upwind-downwind plane, assuming a bulk downwind flow of 20 km s^{-1}. Upwind densities are computed for radiation pressure and ionization values averaged over one year before the observation. Scaling factors have been applied to the data to bring them into agreement with the model. A solar wind asymmetry parameter of A=0.75 has been used. (a) Fit to the upwind data. Data (points) represent the average of three 10° bins centered on the upwind direction. (b) Fit to the downwind data with the same model. Data (points) represent the average of six 10° bins centered on the downwind direction. This model fits both time series but does not simultaneously fit upwind and downwind with the same scale factor. (c) The time series of data divided by model in the upwind direction. (d) The time series of data divided by model in the downwind direction.

It is not entirely clear that we are solving for the physical quantity A in this data set because the look direction is always at -30°.

7. Discussion

A key result in this study is that the downwind brightness is larger than expected at solar maximum and less than expected at solar minimum in a 1-year-average model. We have argued that this is due to the fact that downwind atoms reflect conditions near the Sun in earlier years. A crude model of this effect has improved the fits to the Pioneer Venus Lyman α data. Other workers have argued that such a time dependence is needed. *Blum et al.* [1993] used a Monte Carlo simulation to show that the downwind direction contains a series of hydrogen density waves persisting to hundreds of AU resulting from the time dependence of μ. *Kyrola et al.* [1994], *Rucinski and Bzowski* [1995], and *Summanen* [1996] performed similar calculations showing more modest, but real, density waves that damp rapidly with heliocentric distance. Outer heliospheric models of the downwind hydrogen (Pioneer 10 data) will need to incorporate this effect in the future.

A major assumption in the modeling effort was that the disc-integrated solar line center Lyman α flux, which is responsible for the resonance scattering (and radiation pressure) effects, has a constant line center to line-integrated flux ratio of 0.9, based on initial SOHO SUMER results at solar minimum [*Lemaire et al.*, 1998]. It would be of interest to see if spatially resolved solar Lyman α spectra from the Solar Max Mission (SMM) could be disc-integrated to test this conclusion, as has been done for the O 130.4-nm emission [*Gladstone*, 1992]. Spatially resolved SMM solar Lyman α spectra have a wide variety of shapes, with differing degrees of self-reversal [*Fontenla et al.*, 1988]. Their SMM quiet Sun profiles have a line center to integrated flux ratio of ~1.06. Their SMM active Sun profiles include both larger and smaller ratios. Our successful modeling efforts suggest that the disc-integrated flux and line center flux must be roughly proportional to each other or the

time series data would not track with the model. The cavity shape also depends on this ratio, through the radiation pressure parameter μ. Variations in μ substantially alter the cavity shape and affect our ability to simultaneously fit the data from different longitudes. Our best fitting model parameters should not be considered a unique solution to the problem, as other effects, such as the time dependence of the solar wind latitude asymmetry, may be involved. Solar wind monitoring satellites in the ecliptic do not record solar wind events at high solar latitudes that might change the latitude asymmetry.

The PVOUVS data modeled here only sample one ecliptic latitude (-30°), so they are not particularly well suited for determining the value of A. A primarily affects the downwind brightness and may be a function of time. We found that to simultaneously fit the PVOUVS data obtained over a solar cycle in both the upwind and downwind hemispheres with an SME-based model requires an average value of A=0.5-0.6. Fitting the UARS-based models required a larger value of A=0.75 or more.

Our earlier modeling studies of A used SME-based models. Galileo EUVS Lyman α data from near solar maximum favor a low asymmetry parameter $A\approx0$ [*Pryor et al.*, 1992, 1996]. This result may be compared with A=0.25±0.25 derived from Galileo UVS data from 1990 [*Ajello et al.*, 1994] at solar maximum. Independent work has found A=0.30±0.05 from some special high-latitude PVOUVS observations made during the 1986 encounter with Comet Halley at solar minimum [*Lallement and Stewart*, 1990]. The models are particularly sensitive to A at solar minimum when the solar Lyman α flux is more symmetric [*Ajello* 1990; *Ajello et al.*, 1994]. A companion paper [*Pryor et al.*, this issue] reports evidence from Ulysses interstellar neutral gas (GAS) Lyman α maps that the asymmetry parameter is larger at solar minimum than solar maximum.

The interplanetary Lyman α data can be compared to other measurements of the solar wind asymmetry. Radio observations combined with white light coronagraph observations imply that in going from solar equator to solar pole, the solar wind mass flux (density n_{sw} times velocity v_{sw}) decreases by a factor of 2.3 and solar wind velocity v_{sw} increases by a factor of 2.2 at solar minimum [*Woo and Goldstein*, 1994]. At a typical ecliptic solar wind speed of 350 km s^{-1}, the charge exchange cross section σ is 1.91x10^{-15} cm^{-2}; at a polar wind speed of 350x2.2=770 km s^{-1}, σ falls to 1.30x10^{-15} cm^{-2} [*Barnett et al.*, 1990]. Thus, if the lifetime against charge exchange τ of a hydrogen atom at 1 AU $\tau=1/[n_{sw}\, v_{sw}\, \sigma(v_{sw})]$, then

$$\tau_{pole}/\tau_{equator}$$

$$=[n_{sw}v_{sw}\ \sigma(v_{sw})]_{equator}/[n_{sw}v_{sw}\ \sigma(v_{sw})]_{pole}=2.3(1.91/1.30)=\ 3.37.$$

This ratio corresponds to A=0.70. This estimate is not too different from the UARS-based models evaluated here. Direct solar wind measurements by Ulysses at solar minimum [*Phillips et al.*, 1995] found the median mass flux between -80.2 latitude (September 12, 1994) and 80.2 latitude (July 31, 1995) to be nearly constant with latitude. However, the more relevant quantity for the hydrogen density, the mean mass flux found in these solar wind experiments, decreases by ~40% from equator to pole [*Summanen*, 1996; *Summanen* et al., 1997]. A "harmonic" representation of the Ulysses data (based on the ionization rates of *Summanen et al.* [1997, Figure 2, after subtraction of the photoionization component) would have a solar wind charge exchange lifetime asymmetry factor of A=0.5. The Ulysses measurement is obviously more direct and is in satisfactory agreement with the SME-based Lyman α models discussed here. *Summanen et al.*, [1997] argued that the A representation does not very accurately represent the Ulysses solar wind data, which leads to an ionization rate that is sharply peaked near the ecliptic plane. They find that use of the A representation overestimates the mean ionization rate by 20%. *Pryor et al.*, [this issue] report on different representations for the solar wind mass flux in fitting Ulysses GAS Lyman α maps that are better suited for studying the solar wind asymmetries.

We have attempted to use the best available input parameters in the models, but the uncertainties in some of them remain uncomfortably large. One concern is in the wide range of published densities for hydrogen near the termination shock. The old standard picture favored an inflowing hydrogen gas density of n=0.06-0.08 cm^{-3}. However, "a consensus has been building for a higher hydrogen density" [*Isenberg*, 1997, p. 623] greater than 0.1 cm^{-3}. Our hydrogen density based on our Galileo UVS calibration of n=0.17±0.05 cm^{-3} is a bit higher than average, but the error bar overlaps with the recent pickup ion results of *Gloeckler et al.*, [1997] (n=0.115±0.05 cm^{-3}) and the Lyman α radiation analysis of *Quemerais et al.*, [1994] (n=0.165±0.035 cm^{-3}). Detection of a solar wind slowdown between 1 and 40 AU by *Richardson et al.* [1995] was attributed to a rather low hydrogen density of 0.05 cm^{-3}. However, this low density of 0.05 cm^{-3} requires only a modest multiple scattering correction for an observer at 1 AU from the Sun looking downwind (from sidewind) of ~23% instead of ~35% for n=0.17 cm^{-3} [*Quemerais and Bertaux*, 1993, Table 3] and makes it somewhat harder to reconcile the models with the observed upwind to downwind ratios [*Ajello et al.*, 1994].

A second major concern is the large difference between SME and UARS SOLSTICE solar Lyman α fluxes. *Tobiska et al.*, [1997] use the Pioneer Venus data set from this paper to bridge the gap in time between SME and UARS. As can be seen in Figure 6, there is no large jump in the ratio of the PV data to the model between the end of SME and the beginning of UARS. Differences between the large UARS solar Lyman α irradiance values and smaller SME irradiance values probably reflect absolute calibration differences, as was also found by *Woods and Rottman* [1997] using other solar proxies. *de Toma et al.* [1997] also found a calibration difference between SME and UARS by using Voyager interplanetary Lyman α data to compare the solar measurements.

Using a UARS-based model provides improved agreement with the PV downwind time series data. However, the large radiation pressures in the UARS-based model make the derived asymmetry parameter A somewhat larger than expected from previous work in order to match the observed upwind to downwind ratio. Other factors besides A may contribute to the upwind to downwind ratio. For example, a minor population of superthermal H atoms may act to fill in the downwind cavity. High spectral resolution Hubble Space Telescope (HST) measurements [*Clarke et al.*, 1995] of the hydrogen column between Earth and Mars also indicate an unexpectedly large amount of hydrogen (of noncometary origin) in the downwind cavity. Interplanetary line shape measurements from the Solar Wind Asymmetry (SWAN) experiment on SOHO and the Hydrogen Deuterium Absorption Cell (HDAC) experiment on Cassini may help better characterize the downwind material.

Appendix: Justification for a Model with a "Lagged" Radiation Pressure and Lifetime

First, consider the source function for emission, also known as the volume emission rate. Formally, it is the product of the hydrogen density n, the solar flux, the scattering cross section, and the phase function. We use the standard table of hydrogen densities of *Thomas* [1978] to evaluate the source function. The relative source function for an observer at the Sun is simply the product of density and $1/r^2$, where r is the distance from the Sun in AU. Figure A1 illustrates the relative density and source function. The upwind source function is rather sharply peaked near the maximum emission region, 1-2 AU upwind of the Sun. The downwind source function is rather broad, with substantial contributions from a range of distances. This means that light coming from downwind is being scattered from hydrogen atoms that passed the Sun at various times in the previous few years, when solar conditions were different from the current conditions. We show below that a reasonable first approximation is to model the source function for each downwind volume element using the solar conditions during the year when the hydrogen atoms in that volume element moving at the bulk velocity passed the Sun.

The ionization, radiation pressure, and solar gravity all have a $1/r^2$ dependence. The ratio of the Lyman α radiation pressure force on a hydrogen atom to solar gravity is called μ. Define the effective gravity force $F_g=GMm(\mu\text{-}1)/r^2$ where G is the gravitational constant, M is the mass of the Sun, and m is the mass of a hydrogen atom. Since $\mu\approx1$, the acceleration due to effective gravity is smaller than that due to solar gravity. Finding the trajectory due to effective gravity is analogous to a small angle Coulomb scattering problem [*Nicholson*, 1983). Define θ as the angle between the ray from the Sun in the upwind direction and the ray from the Sun to the atom. Define the impact parameter for an atom moving past the Sun as the closest approach distance p. Then the perpendicular velocity acquired in passing the Sun is

$$v_\perp = \int_{-\infty}^{\infty} \frac{dtF_{g\perp}}{m} = \int_{-\infty}^{\infty} \frac{dtGM(\mu-1)\sin\theta}{r^2} = \int_{-\infty}^{\infty} \frac{dtGM(\mu-1)\sin\theta}{(p/\sin\theta)^2}$$

Let x be the position at time t, given an initial velocity v_0 along the upwind-downwind direction. Assuming the upwind-downwind plane is crossed at t=0, then

$$x = v_0 t = -r\cos\theta = \frac{-p\cos\theta}{\sin\theta} = v_0 t$$

so that

$$dt = \frac{pd\theta}{v_0 \sin^2\theta}$$

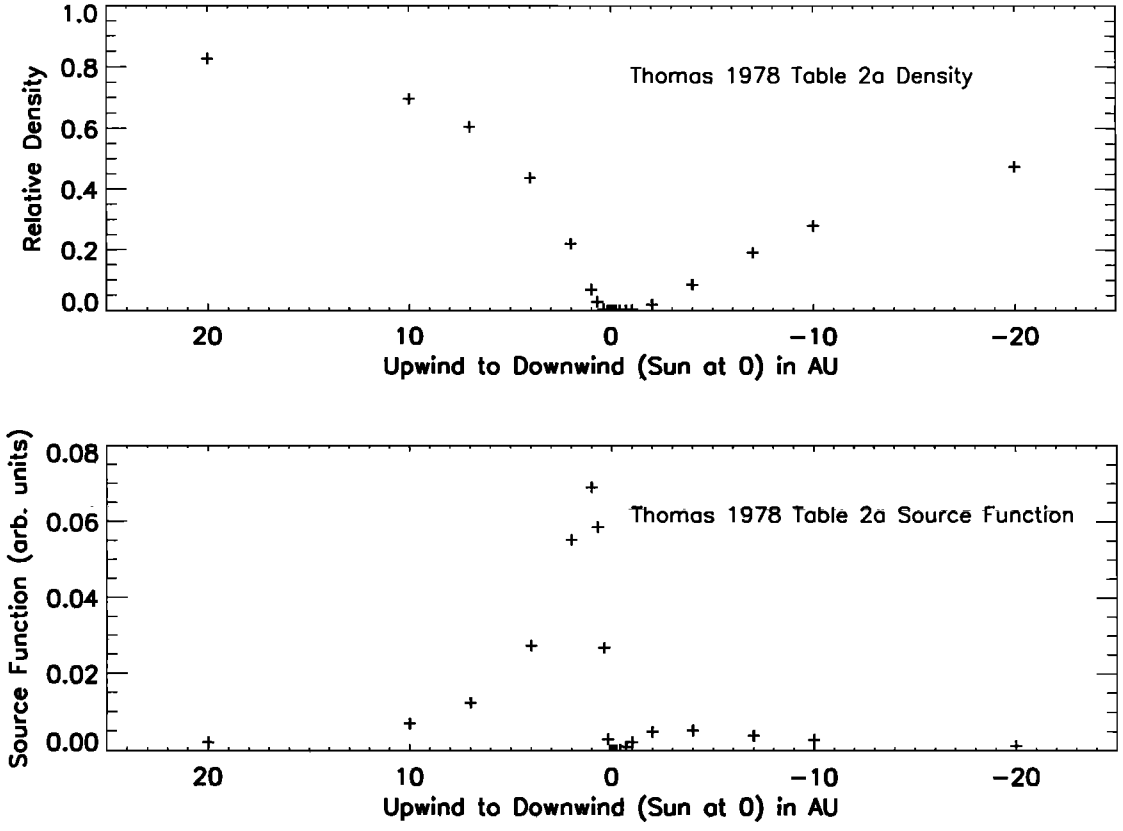

Figure A1. Table 2a of *Thomas* [1978] presents relative hydrogen densities for the case of initial density n=1 cm^{-3}, velocity v=20 km s^{-1}, and temperature T=10,000 K, ionization rate at 1 AU β=5.x10^{-7} s^{-1}, and μ=0.75. (a) The relative densities from that table along the upwind-downwind axis are shown. Upwind is on the left. (b) The relative source function (volume emission rate) is shown in arbitrary units. Note the broad downwind source function.

and finally

$$v_\perp = \frac{GM(\mu-1)}{v_0 p}\int_0^\pi d\theta \sin\theta$$

The last integral numerically equals 2. For atoms traveling at the bulk velocity $v_0 = 20$ km s^{-1}, a distance of 4.2 AU is traveled in 1 year, for example, from 2.1 AU upwind to 2.1 AU downwind in 1 year. Consider an atom with impact parameter p=2.1 AU. In that 1-year interval, θ varies from ~45° to ~135°, if the effective gravity is small. The same integral evaluated from 45° to 135° numerically equals 1.414. In this case, 1.414/2.0=71% of the transverse velocity is acquired in the year of closest approach to the Sun. For atoms with a few AU impact parameter the radiation pressure and effective gravity during the year of closest approach to the Sun control the trajectory.

We also estimate the relative importance of ionization at different distances. This is important for evaluating the right impact parameters p for the preceding estimate: if p is too small, ionization may leave no downwind slow neutral component. A table of interplanetary hydrogen densities presented by *Thomas* [1978, Table 2a) indicates that for an impact parameter of 1 AU, the density at the upwind-downwind plane crossing is only 3% of the initial density. For a 4-AU impact parameter, the density at plane crossing is 30% of the initial density. A few AU seems to be a reasonable estimate for the impact parameter to use in the preceding calculation on transverse velocities. This discussion suggests that a 1-year average of ionization rates and radiation pressures for the period centered on upwind-downwind plane crossing is a useful first approximation to use in evaluating downwind densities at different phases of the solar cycle.

Acknowledgments. This research was supported by the Pioneer Venus Guest Investigator Program, the Space Physics Heliospheric Research Program, the Pioneer Venus Project, the Galileo Project, and the Upper Atmosphere Research Satellite Guest Investigator Program. Fred Lacy and Warren Akers assisted in the preparation of the PV database used here. Alan Lazarus and the NSSDC supplied the necessary solar wind fluxes. Gary Rottman and Barry Knapp provided the SME solar Lyman α database, which includes the solar F10.7 cm fluxes. Jack Harvey's NSO/Kitt Peak He 1083 nm data used here are produced cooperatively by NSF/NOAO, NASA/GSFC, and NOAA/SEL. We acknowledge useful discussions with Tom Woods, Eric Quemerais, Giuliana de Toma, Randy Gladstone, and Bill McClintock.

The Editor thanks two anonymous referees for their assistance in evaluating this paper.

References

Ajello, J. M., Solar minimum Lyman α sky background observations from Pioneer Venus Orbiter ultraviolet spectrometer: Solar wind latitude variation, *J. Geophys. Res., 95*, 14,855-14,861, 1990.

Ajello, J. M., A. I. F. Stewart, G. E. Thomas, and A. Graps, Solar cycle study of interplanetary Lyman alpha variations: Pioneer Venus Orbiter sky background results, *Astrophys. J., 317*, 964-986, 1987.

Ajello, J. M., et al., Simple ultraviolet calibration source with reference spectra and its use with the Galileo orbiter ultraviolet spectrometer, *Appl. Opt., 27*, 890-914, 1988.

Ajello, J. M., W. R. Pryor, C. A. Barth, C. W. Hord, and K. E. Simmons, Solar wind latitude variations and multiple scattering from Galileo interplanetary Lyman α Observations, *Adv. Space Res., 13(6)*, 37-40, 1993.

Ajello, J. M., W. R. Pryor, C. A. Barth, C. W. Hord, A. I. F. Stewart, K. E. Simmons, and D. T. Hall, Observations of interplanetary Lyman α with the Galileo ultraviolet spectrometer: Multiple scattering effects at solar maximum, *Astron. Astrophys., 289*, 283-303, 1994.

Barnett, C. F., ed., *Collisions of H, H_2, He and Li atoms and ions with atoms and molecules*, Oak Ridge Natl. Lab., Rep. ORNL-6086/VI, Vol. 1, Oak Ridge, Tenn., 1990.

Bertaux, J.-L., R. Lallement, V. G. Kurt, and E. N. Mironova, Characteristics of the local interstellar hydrogen determined from PROGNOZ 5 and 6 interplanetary Lyman alpha line, *Astron. Astrophys., 150*, 1-20, 1985.

Blum, P., P Gangopadhyay, H. S. Ogawa, and D. L. Judge, Solar-driven neutral density waves, *Astron. Astrophys., 272*, 549-554, 1993.

Clarke, J. T., R. Lallement, J.-L. Bertaux, and E. Quemerais, HST observations of the interplanetary medium downwind and in the inner solar system, *Astrophys. J., 448*, 893-904, 1995.

Colwell, W., Venus Lyman alpha: A morphological and radiative transfer analysis, Ph.D. dissertation, Univ. of Colo., Boulder, 1997.

de Toma, G., E. Quemerais, and B. R. Sandel, Long-term variation of the interplanetary H Lya glow: Voyager UVS measurements and implications for the solar H Lya irradiance, *Astrophys. J., 491*, 980-992, 1997.

Fontenla, J., E. J. Reichmann, and E. Tandberg-Hanssen, The Lyman alpha line in various solar features, I, Observations, *Astrophys. J., 329*, 464-481, 1988.

Gladstone, G. R., Solar O I 1304-Å triplet line profiles, *J. Geophys. Res., 97*, 19519-19525, 1992.

Gloeckler, G., L. A. Fisk, and J. Geiss, Anomalously small magnetic field in the local interstellar cloud, *Nature, 386*, 374-377, 1997.

Hall, D. T., Ultraviolet resonance scattering and the structure of the heliosphere, Ph.D. thesis, Phys. Dept., Univ. of Ariz., Tucson, 1992.

Hall, D. T., D. E. Shemansky, D. L. Judge, P. Gangopadhyay, and M. A. Gruntman, Heliospheric hydrogen beyond 15 AU: Evidence for a termination shock, *J. Geophys. Res., 98*, 15185-15192, 1993.

Harvey, J. W., Helium 10830 Å irradiance: 1975-1983, in *Solar Irradiance Variations on Active Region Time Scales*, edited by B. J. LaBonte, NASA Conf. Publ., 2310, 197-211, 1984.

Harvey, J. W., and W. C. Livingston, Variability of the solar He I 10830 Å triplet, in *Infrared Solar Physics, IAU Symp. 154*, edited by D. M. Rabin, J. T. Jefferies, and C. Lindsey, pp. 59-64, Kluwer Acad., Norwell, Mass., 1994.

Hord, C. W., et al., Galileo ultraviolet spectrometer experiment, *Space Sci. Rev., 60*, 503-530, 1992.

Isenberg, P. A., Interaction of the solar wind with interstellar neutral hydrogen: Three-fluid model, *J. Geophys. Res., 91*, 9965-9972, 1986.

Isenberg, P. A., A weaker solar wind termination shock, *Geophys. Res. Lett., 24*, 623-626, 1997.

King, J. H., *Interplanetary Medium Data Book*, 77-04, Goddard Space Flight Cent., Natl. Space Sci. Data Cent., Greenbelt, Md., 1977a.

King, J. H., *Interplanetary Medium Data Book*, 77-04A, Goddard Space Flight Cent., Natl. Space Sci. Data Cent., Greenbelt, Md., 1977b.

King, J. H., *Interplanetary Medium Data Book*, 79-08, Goddard Space Flight Cent., Natl. Space Sci. Data Cent., Greenbelt, Md., 1979.

King, J. H., *Interplanetary Medium Data Book*, 83-01, Goddard Space Flight Cent., Natl. Space Sci. Data Cent., Greenbelt, Md., 1983.

Kyrola, E., T. Summanen, and P. Raback, Solar cycle and interplanetary hydrogen, *Astron. Astrophys., 288*, 299-314, 1994.

Lallement, R., and A. I. F. Stewart, Out-of-ecliptic Lyman alpha observations with Pioneer Venus: Solar wind anisotropy degree in 1986, *Astron. Astrophys., 227*, 600-608, 1990.

Lasica, S. J., W. B. Colwell, W. R. Pryor, A. I. F. Stewart, and J. M. Ajello, Solar cycle effect on the Venus Lyman alpha corona, *Bull Am. Astron. Soc., 25*, 1096, 1993.

Lee, M. A., Effects of cosmic rays and interstellar gas on the dynamics of a wind, in *Cosmic Winds and the Heliosphere*, pp. 857-886, edited by J. R. Jokipii, C. P. Sonett, and M. S. Giampapa, Univ. of Ariz. Press, Tucson, 1997.

Lemaire, P., C. Emerich, W. Curdt, U. Schuehle, and K. Wilhelm, Solar HI Lyman α full disk profile obtained with the SUMER/SOHO spectrometer, *Astron. Astrophys., 334*, 1095-1098, 1998.

Nicholson, D. R., *Introduction to Plasma Theory*, John Wiley, New York, 1983.

Ogawa, H. S., C. Y. R. Wu, P. Gangopadhyay, and D. L. Judge, Solar photoionization as a loss mechanism of neutral interstellar hydrogen in interplanetary space, *J. Geophys. Res., 100*, 3455-3462, 1995.

Phillips, J. L., et al., Ulysses solar wind plasma observations from pole to pole, *Geophys. Res. Lett., 22*, 3301-3304, 1995.

Pryor, W. R., J. M. Ajello, C. A. Barth, C. W. Hord, A. I. F. Stewart, K. E. Simmons, W. E. McClintock, B. R. Sandel, and D. E. Shemansky, The Galileo and Pioneer Venus ultraviolet spectrometer experiments: Solar Lyman α latitude variation at solar maximum from interplanetary Lyman α observations, *Astrophys. J., 394,* 363-377, 1992.

Pryor, W. R., et al., Latitude variations in interplanetary Lyman a data from the Galileo EUVS modeled with solar He 1083 nm images, *Geophys. Res. Lett., 23,* 1893-1896, 1996.

Pryor, W. R., M. Witte, and J. M. Ajello, Interplanetary Lyman α remote sensing with the Ulysses Interstellar Neutral Gas Experiment, *J. Geophys. Res.*, this issue.

Puyoo, O., L. Ben Jaffel, and C. Emerich, The neutral hydrogen abundance and ionization in the inner heliosphere, *Astrophys. J., 480,* 262-271, 1997.

Quemerais, E., and J.-L. Bertaux, Radiative transfer in the interplanetary medium at Lyman alpha, *Astron. Astrophys., 277,* 283-301, 1993.

Quemerais, E., J.-L. Bertaux, B. R. Sandel, and R. Lallement, A new measurement of the interplanetary hydrogen density with ALAE/ATLAS 1, *Astron. Astrophys., 290,* 941-955, 1994.

Quemerais, E., B. R. Sandel, R. Lallement, and J.-L. Bertaux, A new source of Ly-α emission detected by Voyager UVS: heliospheric or galactic origin?, *Astron. Astrophys., 299,* 249-257, 1995.

Quemerais, E., Y. G. Malama, B. R. Sandel, R. Lallement, J.-L. Bertaux, and V. B. Baranov, Outer heliospheric Lyman α background derived from two-shock model hydrogen distributions: Application to the Voyager UVS data, *Astron. Astrophys., 308,* 279-289, 1996.

Richardson, J. D., K. I. Paularena, A. J. Lazarus, and J. W. Belcher, Evidence for a solar wind slowdown in the outer heliosphere?, *Geophys. Res. Lett., 22,* 1469-1472, 1995.

Rucinski, D., and M. Bzowski, Modulation of interplanetary hydrogen density distribution during the solar cycle, *Astron. Astrophys., 296,* 248-263, 1995.

Stewart, A. I. F., Design and operation of the Pioneer Venus Orbiter ultraviolet spectrometer, *IEEE Trans. Geosci. Remote Sens., 18,* 65-70, 1980.

Stone, E. C., A. C. Cummings, and W. R. Webber, The distance to the solar wind termination shock in 1993 and 1994 from observations of anomalous cosmic rays, *J. Geophys. Res., 101,* 11,017-11,025, 1996.

Summanen, T., The effect of the time and latitude-dependent solar ionisation rate on the measured Lyman α intensity, *Astron. Astrophys., 314,* 663-671, 1996.

Summanen, T., R. Lallement, and E. Quemerais, Solar wind proton flux latitudinal variations: Comparison between Ulysses in situ data and indirect measurements from interstellar Lyman α mapping, *J. Geophys. Res., 102,* 7051-7062, 1997.

Thomas, G. E., The interstellar wind and its influence on the interplanetary environment, *Annu. Rev. Earth Planet Sci., 6,* 173-204, 1978.

Tobiska, W. K., Revised solar extreme ultraviolet flux model, *J. Atmos. Terr. Phys., 53,* 1005-1018, 1991.

Tobiska, W. K., W. R. Pryor, and J. M. Ajello, Solar hydrogen Lyman α variation during solar cycles 21 and 22, *Geophys. Res. Lett., 24,* 1123-1126, 1997.

Witt, N., P. W. Blum, and J. M. Ajello, Solar wind latitudinal variations deduced from Mariner 10 interplanetary H 1216 A observations, *Astron. Astrophys., 73,* 1979, 272-281, 1979.

Woo, R., and R. M. Goldstein, Latitudinal variation of speed and mass flux in the acceleration region of the solar wind inferred from spectral broadening measurements, *Geophys. Res. Lett., 21,* 85-88, 1994.

Woods, T. N., and G. J. Rottman, Solar Lyman α irradiance measurements during two solar cycles, *J. Geophys. Res., 102,* 8769-8779, 1997.

J.M. Ajello, Jet Propulsion Laboratory, MS 183-601, 4800 Oak Grove Dr., Pasadena, CA 91109.

W.B. Colwell, S.J. Lasica, S. Lineaweaver, W.R. Pryor, D.T. Hall, and A.I.F. Stewart, Laboratory for Atmospheric and Space Physics, 1234 Innovation Drive, University of Colorado, Boulder, CO 80303. (e-mail: wayne.pryor@lasp.colorado.edu)

W.K. Tobiska, FDC/Jet Propulsion Laboratory, MS 264-580, 4800 Oak Grove Dr., Pasadena, CA 91109.

O.R. White, High Altitude Observatory/NCAR, Boulder, CO 80307.

(Received February 10, 1998; revised May 26, 1998;
accepted June 2, 1998.)